

Thermal effects in the size distribution of SiC nanodots on Si(111)

M. Flores^{1,2}, V. Fuenzalida³, and P. Häberle^{*,1}

¹ Departamento de Física, Universidad Técnica Federico Santa María, Av. Los Placeres 401, Casilla 110-V, Valparaíso, Chile

² Instituto de Física, Pontificia Universidad Católica de Valparaíso, Av. Brasil 2950, Casilla 4059, Valparaíso, Chile

³ Departamento de Física, FCFM, Universidad de Chile, Av. Blanco Encalada 2008, Santiago 8370449, Chile

Received 19 December 2004, revised 21 May 2005, accepted 1 June 2005

Published online 26 July 2005

PACS 68.37.Ef, 68.47.Fg, 79.60.Jv, 81.07.–b

We have used scanning tunneling microscopy (STM), Auger electron spectroscopy (AES) and X-ray Photoelectron spectroscopy (XPS) to investigate the formation of nanoscopic structures on Si(111), from wafers with a high bulk C concentration. The samples were prepared by long time thermal annealing of the silicon samples, followed by a high temperature flash in ultrahigh vacuum. An increased surface C concentration is induced by segregation from the bulk. The surface is found to roughen on the nanoscopic length scale, exhibiting a random distribution of nanostructures. The height range of the structures varies between 2 and 20 nm. The size distribution is strongly dependent on the low-temperature preparation conditions. Ex-situ XPS measurements reveal the formation of SiC bonds, thus confirming the nanodots are formed by a surface recombination of SiC.

© 2005 WILEY-VCH Verlag GmbH & Co. KGaA, Weinheim

1 Introduction

The strain-driven formation of three-dimensional ordered islands is a method for building self-assembled structures on semiconductors. It has potential applications in the architecture of novel semiconductor devices [1–3]. In many of these applications the control of the surface roughness, both in the size and spatial distribution of the nanostructures, is essential for the subsequent operation of these arrangements as device. Frequently, the strength of the interaction inducing the self-ordering is limited and therefore methods for enhancing island ordering are being vigorously studied by several techniques, e.g. CVD [4, 5], IBD [6, 7], and MBE [8, 9].

Silicon carbide (SiC) has attracted considerable interest because of its broad potential applications owing much of this new thrust to the fact it is a wide bandgap semiconductor [10–12]. It is well known that semiconductor materials with indirect bandgaps can show the character of a direct optical transition if the material size is decreased to the nanoscale range, where additional quantum confinement effects are dominant [13, 14]. Therefore, the study of SiC at the nanoscale is very meaningful in the application of SiC as part of optoelectronic devices. If the fabrication procedures of nanostructures on Si substrates, based on elements different from C, require high temperatures, care should be taken to minimize the C segregation from the bulk [15, 16], in order to avoid contamination or even the formation of unwanted C induced structures.

* Corresponding author: e-mail: patricio.haberle@usm.cl

In this article we present our results from a study of the size distribution of SiC islands on Si(111) substrates using a UHV-STM. These nanostructures appear after a thermal process in which a Si wafer with a high C bulk concentration is subjected to a time programmed temperature sequence. The migration of the bulk C atoms to the surface, during the annealing process, and the subsequent nucleation give rise to the observed structures. In a recent report [17] on the formation of SiC nano-structures on Si, it has been shown that thermal treatments, in addition to an ordered profile of surface steps, can induce the formation of one dimensional chains of SiC nanostructures. Based on these results, namely, the use of physical constraints such as stepped surfaces, together with sample preparation procedures similar to those described in this report, can prove to be valuable options for the growth of SiC nanostructures.

2 Experimental details

The substrates used were p-type Si(111) wafers (B-doped, resistivity 11–20 Ω cm), with a C concentration higher than usual for a 5N wafer. Before introducing them into the vacuum system, the samples were dipped in methanol and distilled water. In-vacuum preparation and analysis were carried out in a UHV chamber equipped with a commercial scanning tunneling microscope (STM) and a cylindrical mirror analyzer (CMA) for Auger electron spectroscopy. The base pressure of the chamber was below 1×10^{-10} Torr.

Samples were resistively heated overnight (for 12 h), at different temperatures between 660 °C–810 °C, to clean the oxide surface, and later flashed to 1100 °C (~1 min). The temperature was then rapidly reduced to about 850 °C and then they were left to cool down at a rate <2 °C/s [18]. The pressure in the chamber during the 12 h annealing process stayed beneath 4×10^{-10} Torr, and during flashing below 3×10^{-9} Torr. All the STM images were collected with a $V_{\text{bias}} = +2$ V and $I_{\text{tunnel}} = 2$ nA, in a constant current mode. XPS measurements were performed in a separate vacuum system, with an Al anode X-ray source and a spherical electron analyzer. This system also included sputtering gun for the determination of depth profiles.

3 Results and discussion

A typical STM image of the surface we are considering is shown in Fig. 1. This image corresponds to a wafer annealed to 660 °C for 12 h and later flashed to ≈ 1100 °C. The surface is decorated by a distribution of nanodots (ndots), which as we will see below, are mostly SiC. These structures should not be confused with residual contamination from the vacuum system during the annealing process, since the time scale for such accumulation to occur are much larger at the actual operating pressure [19].

Our AES *in situ* measurements shown in Fig. 2 exhibit differences in the C(KLL) peak from this sample (SiC n-dots/Si) when compared to measurements in HOPG, see also Balooch et al. [20]. We have included in the same graph the fresh sample spectrum. It is clear from the differences in the intensities, that C which could have been added by the out of vacuum preparation procedure, is negligible when compared to the strong C signal induced by the thermal treatment. Even though there is not a large shift in the energies of the Auger transitions, the differences in the intensity and shape of the C(KLL) signal

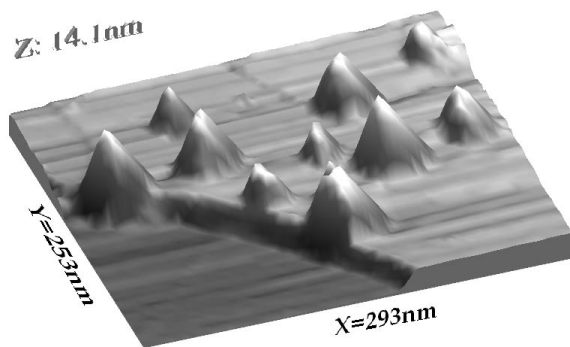


Fig. 1 3D topographic Si surface image, after thermal treatment (long anneal + flash). Area 253 nm \times 293 nm, $V_{\text{bias}} = +2$ V and $I_{\text{tunnel}} = 2$ nA. The picture shows the pointed-shape n-dots.

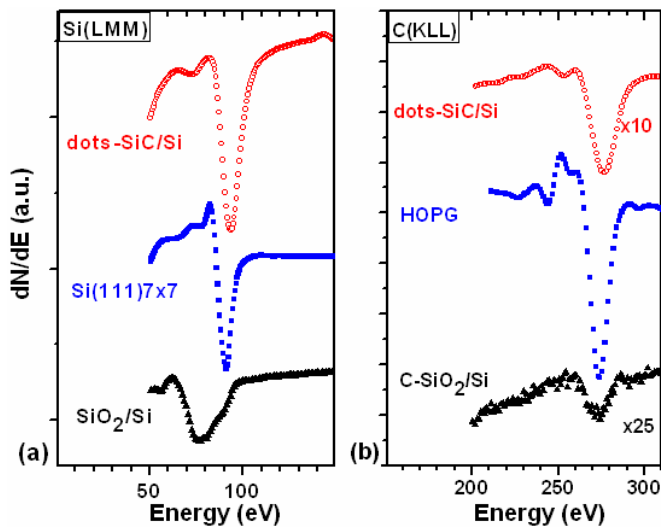


Fig. 2 (online colour at: www.pss-a.com) C and Si Auger signals under different sample conditions. The top traces correspond to measurements after the thermal treatment. The bottom traces are the same signals prior to the treatment. The central spectra correspond to clean Si(111) and HOPG, respectively. (a) From these graphs it is easy to verify the effects of the Si–Si vs. Si–C bonding in the Auger Si signal. We observe a larger FWHM in the surface with the n-dots together with differences in the losses before the main Auger transitions. (b) Similar effects are shown on the main C AES signal.

between HOPG; the Si sample with residual contamination, and the C induced nanostructured surface, is significant enough to suspect a different chemical environment for the C in each case. The Auger signal of the Si(LMM) also presents differences for the different sample conditions (the fresh sample with the native oxide layer (\blacktriangle); the same sample after the thermal treatment (\circ), and a spectrum from the (7×7) reconstruction (\blacksquare) obtained from a high purity sample). These differences in the shape of the Si peak are consistent with C adsorbed in a form different than graphite over the Si surface.

To further explore these qualitative differences, we performed several XPS measurements. We used both a fresh sample and one in which we have induced the formation of the n-dots. In Fig. 3 we show Si 2p and C1s peaks from each one of them. The measurements were performed ex-situ, so the samples were subjected to sputtering to remove some of the effects of the air exposure. The circles correspond to the actual data points, the thick solid line corresponds to the best fit to the data. These lines were obtained by adding the different components contributing to the peaks (narrow lines). From left to right, we show the spectra from: a treated sample (annealed to 760°C + a high T flash), the treated sample after sputtering and a fresh sample (as received from the manufacturer) after sputtering. The fresh sample (c) shows two components in the Si 2p spectrum, one of them originating from the native oxide Si–O at 103.2 eV, and the other from Si atoms in a Si environment (99.6 eV) [22]. The sample in (a), with the n-dots, shows evidence of a Si–C peak, at an energy of 101.3 eV, in addition to the Si–Si 2p peak. Since the sample was taken out of vacuum prior to the XPS measurement, some re-oxidation occurred as shown by the peak at 103.2 eV. After Ar^+ sputtering this sample (b), most of the Si–O peak is removed but the fit of the spectra is improved if we retain the lower energy component (101.0 eV), consistent with Si–C bonding [21].

In Fig. 3(d) to (f), we show the C1s signal for the same samples. The important aspect here is that panels (d) and (e) display unambiguously three peaks associated to the C1s emission. Starting from the lower energy side of the spectrum, shown in panel (d), there is a peak at 283.2 eV, which can be identified with C–Si. The next and most intense peak at 285.4 eV has been labeled as a C–C contribution. A broader and less intense feature at 288.3 eV is required to account for the high energy shoulder displayed by the data. This contribution can be traced back to C–O bonding. The existence of this triple feature in the C 1s spectra explicitly justifies the introduction of a Si–C feature in the fitting of the Si 2p peaks.

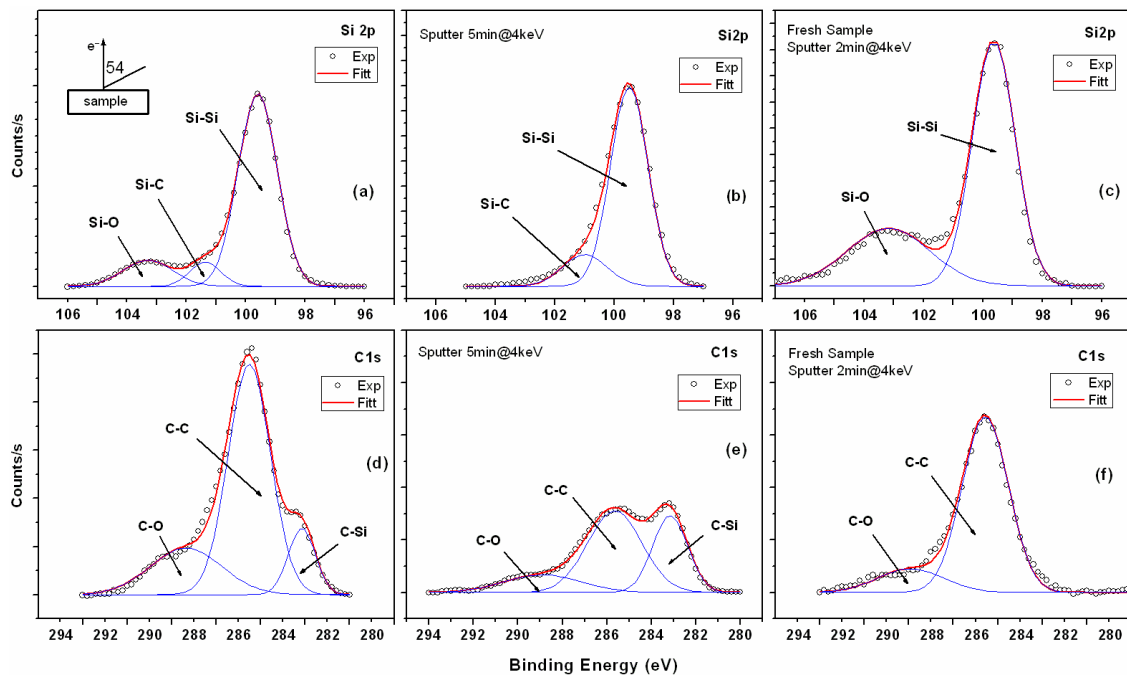


Fig. 3 (online colour at: www.pss-a.com) (a–c) Si2p and (d–f) C1s spectrum from surface: (a) and (d) after a long anneal (760 °C) + high T flash; (b) and (e) same sample as in (a) after Ar sputtering; (c) and (f) a sputtered Si(111) sample. The open circles are experimental data points, the solid lines are the best fit curve. Note that Si–O and C–O are present in spectrum (a) and (d), respectively, since the sample was exposed to air before performing the XPS measurements. To compare these spectra in the same terms we have taken out the shift due to charging using spectrum (b) as a reference to fix the Si–Si energy at ~ 99.6 eV. The other spectra in this figure have been shifted accordingly.

The effect of sputtering in this sample is to remove a large fraction of the C–C intensity but the triple peak of the C1s is still clearly observable. These 2 panels, (d) and (e), should be compared with (f), which is an XPS spectrum from a sputtered Si sample (no heat treatment). In this sample we only detect a double feature, namely a contribution from the surface C–C contamination and a second one from the oxide formation (C–O bonding). The leading edge, displayed by the C 1s feature in the sample with the n-dots at 283.2 eV (d), is absent in this case, as it should be, since no Si–C formation is expected in this case. Since the sputtering process modifies the surface charging, a useful and charge-independent parameter is the energy difference between the C1s and Si2p associated to carbides. We have labelled them as C1s(Si) and Si 2p(C). This difference in binding energy, $\Delta BE[C1s(Si) - Si2p(C)] \approx 182.2$ eV, in our data. This value, which remained constant independent of the time span of the erosion cycles, has been previously identified as originating from SiC [21]. Similar results were obtained for other samples treated at different temperatures. The main conclusion which could be drawn from these XPS data is that the thermal treatment applied to the high C content Si substrates, induces the formation of SiC on the surface.

The set of STM images shown in Fig. 4 corresponds to a series of samples subjected to different overnight annealing temperatures (for a time length of 12 h) and subsequently flashed to 1100 °C. There is a clear evolution of the surface structure depending on the temperature. One common aspect to all of these images is the presence of atomic steps between flat terraces. Most of these steps, which follow curved patterns, are pinned to the SiC n-dots and they are distributed over the surface with no particular orientation. We believe the pattern of the steps are influenced both, by the SiO desorption process together with the formation of the SiC n-dots [7]. Another interesting observation from this set of images is the temperature dependence of the dots distribution. Since all of the images shown correspond to samples which

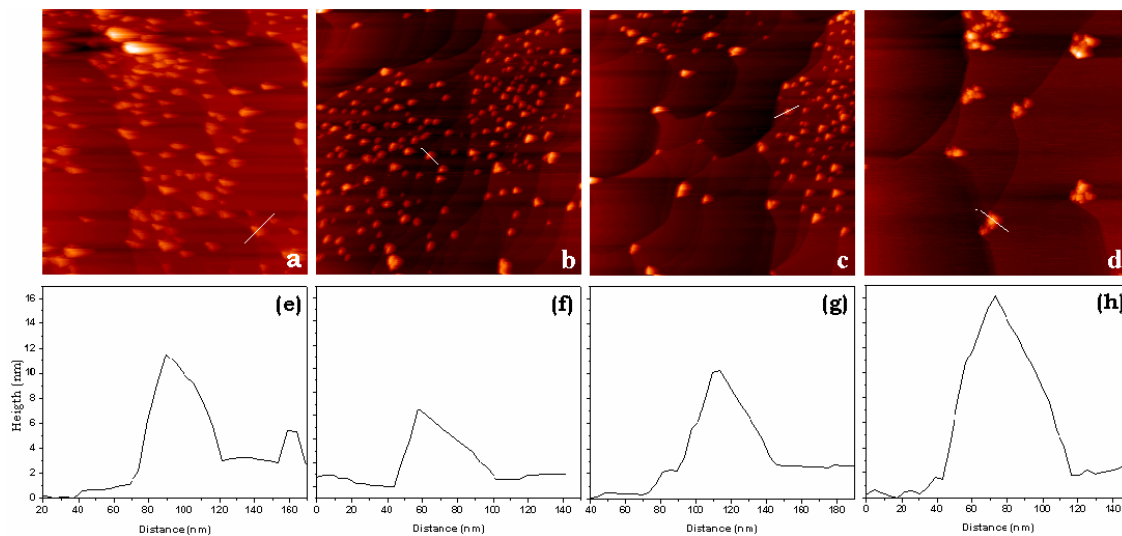


Fig. 4 (online colour at: www.pss-a.com) Topographic image series of samples subjected to different overnight annealing temperatures: (a) 660 °C, (b) 715 °C, (c) 760 °C and (d) 810 °C, prior to the same high temperature flash for all samples. The scanned areas are the same for all the images: 1000 nm × 1000 nm, $V_{\text{bias}} = +2$ V and $I_{\text{tunnel}} = 2$ nA. The line profiles (e–f) correspond to a particular dot in the figures above.

have been annealed to 1100 °C, the macroscopic surface structure retains some of the features present in the surface previous to this last thermal process. There is a higher density of n-dots for the lower overnight annealing temperature. As the temperature increases, further clustering occurs and hence there is an apparent net loss of “C induced defects”, or equivalently, a decrease in the number of n-dots per unit area. It should also be noted that, from the images shown, only the sample in Fig. 4(d), as confirmed by AES measurements, has been pre-annealed well above the SiO desorption temperature. Higher overnight temperatures were also tried with the purpose of inducing the n-dots with negative results. Namely, we observed (images not shown here) the formation of large clusters with no particular shape or length scales, thus confirming in part that the reduction of the density of dots is linked to the coalescence of the smaller size structures.

We systematically performed STM measurements in smaller size areas over the flat sections between the n-dots. Most of the time we obtained atomic resolution over flat areas and the samples exhibited a (7×7) surface reconstruction.

Figure 5 shows a series of volume and height distribution plots measured at room temperature. The size of the structures varies between 2 and 20 nm for temperatures in the range 660 to 810 °C. There are changes in the size distribution of the islands, depending on the initial annealing temperature. We have adjusted a Gaussian distribution for the height at the low temperature range. The height distribution is narrower and centred almost at the same height for the temperatures 715 °C y 760 °C (5.8 nm and 6 nm respectively).

For temperatures of 660 °C and 810 °C the distributions are wider, and in the later case the roughness occurs over a different surface length scale, making it impossible to fit the roughness by a distribution over a 1000×1000 nm² region.

An indication that the shape of the n-dots remains constant under the different annealing temperatures is given by the power law relating the volume with the base surface area of the n-dots. If the length scales in the 3 dimensions are similar, then is reasonable to describe the Volume (V) as proportional to the Area (A) to the $3/2$ exponent ($V \sim A^{3/2}$). We have measured this exponent from the log (volume) vs. log (area) plots shown in Fig. 5. The exponent (ε) is very close to $3/2$ for all cases with the largest discrepancy being $\varepsilon = 1.25$; for 715 °C.

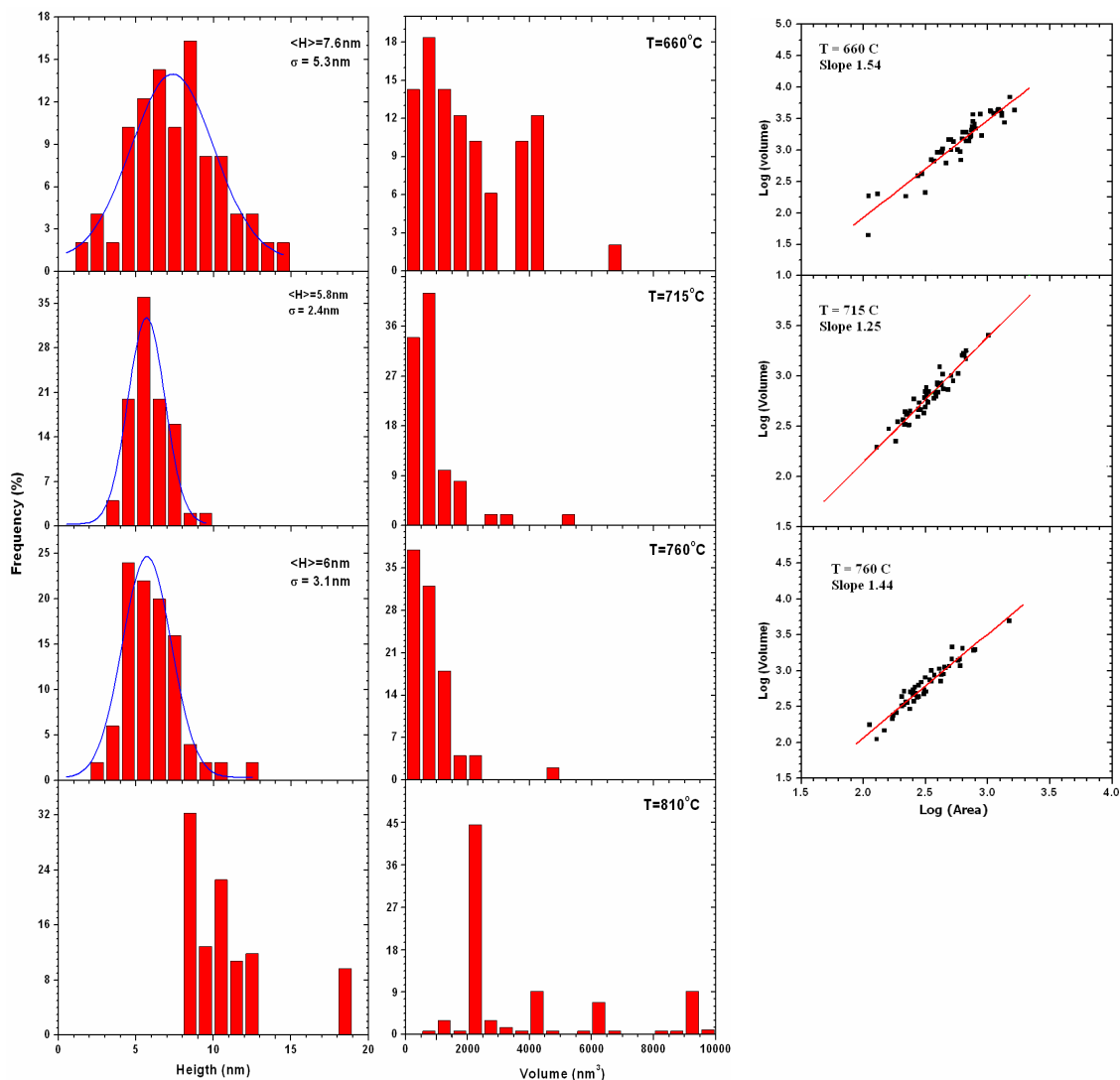


Fig. 5 (online colour at: www.pss-a.com) First two columns of this figure show height and volume histograms for Si samples treated at different annealing temperatures. The graphs at the extreme left show the log (volume) vs. log (area) plots for the corresponding temperatures. The slope is $\approx 3/2$ for all temperature values.

The shape of the SiC structures is reminiscent of Ge nanocrystals grown on Si [4]. Even though our STM images do not have enough resolution to distinguish facets or preferential orientation of the n-dots with respect to the substrate, the shape of the particles is consistent with nanocrystalline pyramids or domes. Further higher resolution measurements are necessary to clarify if this is indeed the case.

The evidence presented here confirms the formation of SiC n-dots induced by C segregation from the bulk. Upon condensation, the two phases present in the surface (Si and SiC) segregate to form the observed distribution of n-dots. From our AES and specially XPS measurements of the Si 2p and C 1s features, we can state that an important fraction of the C atoms in the surface are bound to Si. Furthermore the C detected on the surface concentrates mostly on the n-dots, since the regions in between them, display the (7×7) reconstruction of a clean Si(111) surface. A previous XPS report of C adsorption on Si [22], shows that most C atoms remaining on the surface, after annealing to temperatures comparable to those used in our experiment, are in the form of SiC. Nevertheless, our ex-situ XPS measurements

show evidence of C–C bonding, which accordingly, we attribute to the exposure of the sample to ambient conditions.

There are at least four different thermally activated processes that take place in our samples during the thermal treatments. The first one relates to the migration of C to the surface, the second one is the SiO desorption, which removes the native oxide by the formation of large voids in the first surface layer [23]. The last two, which most likely occur simultaneously, are the clustering of SiC and the formation of the (7×7) reconstruction over the C free sections of the surface.

One singular aspect of our results is the existence of a high temperature limit for the long time thermal annealing. If the temperature goes beyond the SiO desorption threshold (810 °C), the distribution of SiC n-dots is strongly modified. Neither the shape, nor the spatial distribution could be related to the lower temperature data. Our STM images show the formation of large SiC clusters with no particular shape, in contrast to what it is observed at lower temperatures, where a uniform distribution of pointed-shape n-dots is obtained. Even though the temperature and hence the atomic displacements are very large during the high temperature flash, the C distribution seems to retain some features from the previous low temperature anneal. In this way, the final density of C induced dots could be controlled, within a certain range of temperatures, in the thermal process.

4 Summary

In this study, SiC n-dots were prepared on a Si(111) substrate by segregation of carbon atoms from the bulk. The height of the clusters varies between 2 and 20 nm, and the size distributions are fairly sharp. The n-dots have a pointed shape, up to the clustering temperature. Furthermore, the resulting atomic steps in the surface are pinned to the n-dots and follow the characteristic curved patterns formed during SiO desorption. The formation of these n-dots distribution through diffusion, nucleation and recombination of SiC, occurs in a fairly long time scale. Some features of the n-dot distribution are retained after the high temperature anneal in which the (7×7) reconstruction is formed over the C-free sections of the surface.

Acknowledgements This research has been possible due to the partial support of the following grants: MECESUP, FONDECYT, Fundación Andes and ICM (P02-054-F), Chile, together with EU grant CII*-CT93-0059.

References

- [1] V. A. Shchukin and D. Bimberg, *Rev. Mod. Phys.* **71**, 1125 (1999).
- [2] R. Loo, P. Meunier-Beillard, D. Vanhaeren, H. Bender, M. Caymax, W. Vandervorst, D. Dentel, M. Goryll, and L. Vescan, *J. Appl. Phys.* **90**, 2565 (2001).
- [3] B. Voigtländer, *Surf. Sci. Rep.* **43**, 127 (2001).
- [4] M. Goryll, L. Vescan, K. Schmidt, S. Mesters, H. Lüth, and K. Szot, *Appl. Phys. Lett.* **71**, 410 (1997).
- [5] G. Capellini, L. Di Gaspare, F. Evangelisti, and E. Palange, *Appl. Phys. Lett.* **70**, 493 (1997).
- [6] B. Pécz, H. Weishart, V. Heera, and L. Tóth, *Appl. Phys. Lett.* **82**, 46 (2003).
- [7] Y. Xu, K. Narumi, K. Miyashita, and H. Naramoto, *Surf. Interface Anal.* **35**, 99 (2003).
- [8] V. Cimalla, K. Zekentes, and N. Vouroutzis, *Mater. Sci. Eng. B* **88**, 186 (2002).
- [9] F. Sharmann, P. Maslarski, W. Attenberger, J. K. N. Lindner, B. Stritzker, Th. Stauden, and J. Pezoldt, *Thin Solid Films* **380**, 92 (2000).
- [10] A. Kassiba, M. Makowska-Janusik, J. Bouclé, J. F. Bardeau, A. Bulou, and N. Herlin-Boime, *Phys. Rev. B* **66**, 155317 (2002).
- [11] X. L. Wu, G. G. Siu, M. J. Stokes, D. L. Fan, Y. Gu, and X. M. Bao, *Appl. Phys. Lett.* **77**, 1292 (2000).
- [12] S. Kerdiles, A. Berthelot, R. Rizk, and L. Pichon, *Appl. Phys. Lett.* **80**, 3772 (2002).
- [13] M. S. Hybersten and M. Needels, *Phys. Rev. B* **48**, 4608 (1993).
- [14] Y. Kanemitsu, H. Uto, Y. Masumoto, and Y. Maeda, *Appl. Phys. Lett.* **61**, 2187 (1992).
- [15] P. Werner, H. Grossmann, D. Jacobson, and U. Gösele, *Appl. Phys. Lett.* **73**, 2465 (1998).
- [16] Y. J. Kim, T. J. Kim, T. K. Kim, B. Park, and J. H. Song, *Jpn. J. Appl. Phys.* **40**, 773 (2001).
- [17] V. Cimalla, A. A. Schmidt, Ch. Foester, K. Zekentes, O. Ambacher, and J. Pezoldt, *Superlattices Microstruct.* **36**, 345 (2004).

- [18] B. S. Swartzentruber, Y. M. Mo, M. B. Wedd, and M. G. Lagaly, *J. Vac. Sci. Technol. A* **7**, 2901 (1989).
- [19] F. Xie, P. Von Blankenhagen, J. Wu, J. Liu, Q. Zhang, Y. Chen, and E. Wang, *Appl. Surf. Sci.* **181**, 139 (2001).
- [20] M. Balooch, R. J. Tench, W. J. Siekhaus, M. J. Allen, A. L. Connor, and D. R. Olander, *Appl. Phys. Lett.* **57**, 1540 (1990).
- [21] Y. Mizokawa, K. M. Geib, and C. W. Wilmsen, *J. Vac. Sci. Technol. A* **4**, 1696 (1986).
The NIST X-ray Photoelectron Spectroscopy (XPS) Database (<http://srdata.nist.gov/xps/intro.htm>) (2004).
- [22] K. Sakamoto, D. Kondo, Y. Ushimi, M. Harada, A. Kimura, A. Kakizaki, and S. Suto, *Phys. Rev. B* **60**, 2579 (1999).
- [23] D. Jones and V. Palermo, *Appl. Phys. Lett.* **80**, 673 (2002), and references therein.